SUPPRESSED DISASSEMBLY OF AUTOLYZING p94/CAPN3 BY N2A CONNECTIN/TITIN IN A GENETIC REPORTER SYSTEM*

Yasuko Ono[1], Fukuyo Torii[2], Koichi Ojima[1,3], Naoko Doi[1,3], Katsuhide Yoshioka[2], Yukiko Kawabata[2,3,§], Dietmar Labeit[4], Siegfried Labeit[4], Koichi Suzuki[5], Keiko Abe[2], Tatsuya Maeda[3,6], and Hiroyuki Sorimachi[1,3]

From [1]Department of Enzymatic Regulation for Cell Functions, The Tokyo Metropolitan Institute of Medical Science (Rinshoken), Tokyo 113-8613, Japan, [2]Graduate School of Agricultural and Life Sciences, The University of Tokyo, Tokyo 113-8657, Japan, [3]CREST, Japan Science and Technology (JST), Saitama 332-0012, Japan, [4]Institut für Anästhesiologie und Operative Intensivmedizin, Universitätsklinikum Mannheim, Mannheim 68167, Germany, [5]New Frontiers Research Laboratories, Toray Industries Inc., Kanagawa 248-8555, [6]Institute of Molecular and Cellular Biosciences, The University of Tokyo, Tokyo 113-0032, Japan,[§]Present address: Department of Applied Biological Science, Fukuyama University, Hiroshima 729-0292, Japan

Running title: Regulation of p94/calpain 3 stability by N2A connectin/titin

Address correspondence to: Hiroyuki Sorimachi, Department of Enzymatic Regulation for Cell Functions, The Tokyo Metropolitan Institute of Medical Science (Rinshoken), 3-18-22 Honkomagome, Bunkyo-ku, Tokyo 113-8613, Japan, Tel./Fax. +81-3-3823-2181; E-Mail: sorimach@rinshoken.or.jp

p94/calpain 3 is a skeletal muscle-specific member of the Ca^{2+}-regulated cytosolic cysteine protease family, the calpains. Defective p94 protease activity originating from gene mutations causes a muscular dystrophy called calpainopathy, indicating p94's indispensability for muscle survival. Because of the existence of the p94-specific regions IS1 and IS2, p94 undergoes very rapid and exhaustive autolysis. To elucidate the physiological relevance of this unique activity, p94's autolytic profiles and the effect of the p94 binding protein, connectin/titin, on this process were investigated. *In vitro* analysis of p94 autolysis showed that autolysis in IS1 proceeds without immediate disassembly into fragments, and that the newly identified cryptic autolytic site in IS2 is critical for disassembling autolyzed fragments. As a genetic system to assay p94 autolysis semiquantitatively, p94 was expressed in yeast as a hybrid protein between the DNA binding and activation domains of the yeast transcriptional activator Gal4. Transcriptional activation by the Gal4–p94:WT hybrid protein is precluded by p94 autolysis. Complete or partial loss of autolytic activity by C129S active-site mutation, LGMD2A pathogenic missense mutations, or PCR-based random mutagenesis could be detected by semiquantitative restoration of Gal4-dependent β–galactosidase gene expression. Using this system, the N2A connectin fragment that binds to p94 was shown to suppress p94 autolytic disassembly. The proximity of the IS2 autolytic and connectin-binding sites in p94 suggested that N2A connectin suppresses IS2-autolysis. These data indicate the importance of p94–connectin interaction in the control of p94 functions by regulating autolytic decay of p94.

Calpains (named after the first-discovered and best characterized member, Ca^{2+}-dependent and papain-like protease, EC 3.4.22.18, clan CA, family C2) correspond to a diverse gene family whose members all share the characteristic "calpain protease domain", and comprise a unique branch of the cysteine proteases (1,2). To date, calpains have been identified in many different mammalian tissues and in almost all types of living organism (3).

Studies on calpain protease activity, from enzymatic characterization to clarification of its roles in cellular phenomena, have mainly advanced knowledge of the conventional calpains, the μ- and m-calpains. These ubiquitously expressed calpains can be conveniently assayed *in vitro* using established and reproducible methods, such as casein hydrolysis assay, facilitating development of more specific inhibitors as well as more sensitive substrates.

In contrast, the skeletal-muscle-specific calpain, p94/calpain 3, has remained poorly characterized

with regard to its protease activity. The expression of p94 predominates over other calpain species in skeletal muscle, and a defect in p94 proteolytic activity originating from gene mutations causes muscular dystrophy (4-6). In this context, p94 exemplifies the critical importance of tissue-specific calpain species that must fulfill unique functions, thereby, necessitating innovative approach to investigate.

One characteristic of p94 is its very rapid and exhaustive autolytic activity, making it unfeasible to carry out *in vitro* activity assays using purified p94 protein (7). Previously, we took advantage of the relatively stable nature of one of the splice variants of p94, p94Δ, determined enzymatic profiles, protease inhibitor sensitivity *in vitro*, and found that calpastatin, an endogenous inhibitor protein specific to calpains, is a substrate for p94 (8). p94Δ lacks p94-specific insertion sequences, the IS1 and IS2 regions, encoded by exons 6 and 15/16, respectively, and it is feasible to carry out expression and purification of recombinant product at a scale sufficient for biochemical analysis. Another group has also shown that the bacterially expressed protease core of p94 serves as a useful enzyme source for *in vitro* kinetic analysis (9,10). Furthermore, a clan of alternatively spliced forms of p94, which is expressed in rodent lenses, was also shown to be useful for *in vitro* enzymatic study (11). Together, these data strongly attribute the apparent autocatalytic instability of p94 to IS1 and IS2.

There is an interesting discrepancy between recombinantly expressed p94 protein and native p94 protein in skeletal muscle. Although too unstable to completely purify (12), the full-length p94 protein can be detected in freshly prepared skeletal muscle homogenates (13,14) in contrast to recombinantly expressed p94, which is mainly detected as autolyzed fragments (7). Therefore, it is predicted that skeletal muscle cells keep p94 from undergoing autolysis constitutively or randomly. One of the candidate molecules regulating p94 stability is connectin/titin, a gigantic sarcomeric protein in striated muscle. In both skeletal and cardiac muscles, a single connectin molecule extends from the Z-line to the M-line and therefore spans the entire half-sarcomeric distance of more than 1 μm. Previously, our yeast two-hybrid studies showed that p94 binds to two distinct regions, the N2A and C-terminus regions, of connectin, which are located in the sarcomeric N2- and M-lines, respectively (15,16); "A" in N2A represents a splice variant predominant in skeletal muscle. In accordance with this, p94 has been immunolocalized to the N2- and M-line regions in the skeletal muscle sarcomere (17). The biochemical properties of p94 from skeletal muscle present features of connectin-bound proteins, *i.e.*, p94 is enriched in the connectin-rich saline-insoluble fraction. Isolation of p94 from this myofibril fraction provokes rapid autolysis and disappearance of full-length p94 protein (12). It was recently established that an in-frame deletion in the connectin N2A region causes a recessively inherited severe muscular dystrophy in mice: muscular dystrophy with myositis, *mdm* (18). The deletion caused by *mdm* results in a loss of p94-interacting activity of N2A connectin in the yeast two-hybrid system, and the amount of p94 protein shows a tendency to decrease in *mdm*/*mdm* skeletal muscle (19,20). Together, these observations support the hypothesis that binding to connectin is related to p94 stability. However, the actual interaction between p94 and the N2A connectin fragment has not yet been studied under the physiological context. Therefore, the significance of the interaction between p94 and N2A connectin and of the loss of interaction between p94 and *mdm*-type N2A connectin requires further investigation.

The focus of this study was to monitor the autolytic activity of p94 and to evaluate the factor(s) affecting this activity. We used the yeast transcriptional activator Gal4 system, which was originally described as "proteinase trapping" (21), to measure the autocatalytic activity of several viral proteases such as the 3C protease of coxsackievirus B3, the 2A protease of poliovirus, and the human immunodeficiency virus protease (22-24). In our system, suppression of p94 autolytic activity was detected as an increase in transcriptional activation using a hybrid protein of two functional domains of Gal4 (Gal4bd and Gal4ad) linked by p94. This is the first example in which a mammalian protease is applied to proteinase trapping. Using this methodology in combination with other *in vitro* analyses has been beneficial in revealing the autolytic processes of p94. This genetic system also could be used for examining the effect of wild type and *mdm*-type connectin fragments on p94 autolysis, and

profiling structure–function relationships underlying autolytic/protease activity unique to p94.

EXPERIMENTAL PROCEDURES

cDNA constructs – The cDNAs for human and mouse p94/calpain 3 were kind gifts from Drs. Muriel Herasse and Isabelle Richard. The cDNA corresponding to the C-terminal transcriptional activation domain (AD) of Gal4 was isolated from pACT2, a yeast expression vector provided in the MATCHMAKER Two-Hybrid System (Clontech, CA, USA), and was subcloned into pAS2-1C, which encodes the Gal4 DNA binding domain (BD), in tandem with human p94, resulting in the BD–p94–AD-expressing vector. Human connectin cDNA clones CN48 and CN52, encoding N2A and C-terminal regions of connectin, respectively, have been reported previously (16). The mouse cDNA corresponding to the human connectin CN48 clone (nt. 28858-29769 of NM_133378) was amplified by PCR from mouse skeletal muscle cDNA using *Pfu* DNA polymerase (Stratagene, CA, USA). The mammalian expression vector pcDNA3.1/N-FLAG and the yeast expression vectors pAS2-1C, p415GPD, and p425GPD have been described elsewhere (25). Human and mouse p94 cDNAs were constructed into pSRD for protein expression under the SRα promoter, as previously described (6,26). Mouse p94 (wild type or a splice variant without exon 6) was also tagged with tandem myc and 6×His epitopes at the C-terminus. Mutagenesis using long PCR with *Pfu* or *Pfu*-Turbo DNA polymerases was performed to introduce all the mutations, as previously described (6). p94:N358D was constructed by introducing an Asn358 to Asp mutation into the human p94 cDNA and inserting this into the *Bam*HI–*Kpn*I sites of the pFastBac-HTb vector (Invitrogen, CA, USA), which adds 6×His at the N-terminus. Enzymes used for manipulating recombinant DNA were purchased from Takara Bio (Kyoto, Japan) or New England Biolabs (MA, USA). All constructs were verified by DNA sequencing.

Yeast transformation and assay for reporter gene expression – Saccharomyces cerevisiae strains, AH109 and CG1945, were transformed using the Fast^{TM}-Yeast Transformation Kit (Gene Technology, MO, USA), according to the protocol provided by the manufacturer. Transformants were selected on plates with SD-medium that lacked Trp (described as SD-W), or SD-LW. The expression of reporter genes *HIS3*, *ADE2*, or both was assessed by colony growth of AH109 on SD-LWH, SD-LWA, or SD–LWHA plates, respectively. Expression of the reporter gene *lacZ* was evaluated using CG1945 by liquid culture assay for β-galactosidase activity using ONPG as a substrate. All the procedures were carried out following the "Yeast Protocols Handbook" (PT3024-1, Clontech) with some modifications. One unit of β-galactosidase activity corresponds to 1 μmol of ONPG hydrolyzed per min at 30°C. The amount of yeast cells per reaction as well as the reaction time was adjusted so that the measured A_{420} value remains within the linear range of the assay.

Random mutagenesis by PCR – Random mutations were introduced using human wild-type p94 cDNA and the primers, 5′–ATA CAT ATG CCG ACC GTC ATT AGC GC–3′ and 5′–ATG TTG ATG TAG GTT TTG CTC C–3′, which correspond to NS and domain III of p94. The reaction was performed in 50 μl of the solution [0.2 mM dGTP, 1 mM dATP/dCTP/TTP, 400 nM of each primer, 3 mM $MgCl_2$, 0.5 mM $MnCl_2$ in 1 × rTaq buffer (Takara Bio)] with 50 ng of template DNA (human wild-type p94 cDNA) and 1.25 units of rTaq using the following cycles: 94°C, 5 min; [94°C, 30 sec; 55°C, 30 sec; 72°C, 120 sec] × 25 cycles; 72°C, 7 min. However, these conditions turned out to be too mutation prone, and in the second set of experiments, the reaction was performed under "normal" PCR conditions, ***i.e.***, in 50 μl of the solution [0.2 mM dGTP/dATP/dCTP/TTP, 500 nM of each primer in 1 × ExTaq buffer containing 2 mM Mg^+ (Takara Bio)] with 50 ng of template DNA and 1.25 units of ExTaq (Takara Bio) using the same cycles as above. The mutagenized cDNA fragments (20 μg) were cotransformed with 20 μg of the 6.7 kb *Tth*111I–*Psh*AI fragment of the BD–p94–AD expression vector into AH109 to cause *in vivo* ligation by homologous recombination, as previously described ((27), see Fig. 4A). About 2 × 10^6 transformant were screened on selection medium plates, SD–WHA, yielding about 3,400 colonies. Plasmid DNA was isolated from these colonies, and mutations were identified by DNA sequencing.

In vitro autolytic assay using recombinant protein – *Spodoptera frugiperda* cells (Sf-9) were generously provided by Dr. Takeshi Nishino (Nippon Medical School, Tokyo, Japan). Recombinant p94:C129S and p94Δ were expressed and purified as previously described (8). N-terminally His-tagged p94:N358D was expressed in the Sf-9/baculovirus system in the same manner and purified using a His-Bind Quick 900 Ni^{2+}-affinity column cartridge (Takara Bio) according to the manufacturer's instructions. Briefly, 5×10^7 infected Sf-9 cells were homogenized by sonication in 2 ml of 20 mM Tris-HCl, pH 7.5, 5 mM $NaHCO_3$, 0.1 mM EGTA, 1 mM PMSF, and 5 mM 2-mercaptoethanol. After supercentrifugation, the supernatant was applied to the His-Bind Quick 900 cartridge preequilibrated with 1 mM His in buffer A (20 mM Tris-HCl, pH 7.5, 0.5 M NaCl, 5 mM 2-mercaptoethanol). The cartridge was washed with 10 ml of 1 mM His in buffer A, and eluted with 2.5 ml of 0.2 M His in buffer A. The eluent was immediately desalted by applying it to a PD-10 gel filtration column (Amersham Biosciences, NJ, USA) preequilibrated with 10 mM Tris-HCl, pH 7.5, 5 mM EDTA, and 1 mM DTT, and used for experiments within a few days. Protease-inactive p94:C129S (final 1 mg/ml) and the splice variant p94Δ were mixed at a molar ratio of 10:1 and incubated at 37°C for up to 240 min. The assay solution contained 0.1 M Tris/Cl, pH 7.5, 25 mM 2-mercaptoethanol, and 25 mM Ca^{2+}. Autolysis of p94:N358D was performed by incubating it in 50 mM Tris-HCl, pH 7.5, 0.5 M NaCl, 1 mM DTT, 1 mM PMSF, 1 μM pepstatin A, and 10 μM TLCK at 37°C (p94:N358D protein: final 10 μg/ml). The reaction was terminated at the indicated times by the addition of 5 × sample buffer followed by 5 min incubation at 95°C. The 0 min sample was constituted by adding each component into a tube that already contained sample buffer.

SDS-PAGE and native-PAGE analyses – Proteolytic fragments were subjected to SDS- or native-PAGE followed by CBB-staining and western blotting. SDS-PAGE was performed according to the standard Laemmli method using 10% gels. Native-PAGE analysis was carried out essentially in the same manner but without SDS, and electrophoresed by a constant current 5-10 mA at 4°C. Scanned images of CBB-stained gels were converted for densitometric evaluation. The outline of each band was defined by the sharpness of the contrast against background. The amount of protein in each band was represented by volume OD and normalized against the value at 0 min of incubation set to 1.

Protein expression in COS7 cells for western blotting and immunoprecipitation – COS7 cells were cultured in Dulbecco's modified Eagle's medium supplemented with 10% fetal calf serum heat inactivated prior to use (56°C, 30 min). Electroporation was performed using a Bio-Rad gene pulser, according to the manufacturer's instructions. Cells were harvested 72 hr after electroporation and sonicated in a solution consisting of 100 mM Tris-HCl, pH 7.5, 10 mM EDTA, and 1 mM dithiothreitol, as previously described (6). After SDS-PAGE, proteins were transferred to PVDF membranes (Millipore, Tokyo, Japan), which were, then, probed with appropriate primary antibodies and horseradish peroxidase-coupled secondary antibodies followed by visualization using POD immunostaining kit (Wako, Osaka, Japan).

For immunoprecipitation, cells transfected with expression constructs for mouse p94 with or without a C-terminal myc-His tag were harvested in lysis buffer (50 mM Tris-HCl, pH 7.5, 0.15 M KCl, 1 mM EDTA-K, 1% (v/v) NP40, and 0.5% Triton X-100) containing protease inhibitors as follows: 1.5 μM aprotinin, 1 mM PMSF, 50 μM leupeptin, 50 μM TLCK, and 2 mM iodoacetoamide. After 30 min on ice with occasional tapping, the lysate was centrifuged at 11,000 × *g* for 10 min, and the supernatant was used for immunoprecipitation using anti-pIS2 or anti-myc antibodies.

The antibodies used in this study included a p94-specific anti-pIS2 antibody raised in goat against the epitope identical to the one used for the previously described anti-pKrich (7), an anti-pNS antibody (7), an anti-dIII antibody (Triple Point Biologics, OR, USA, RP3-calpain3), a mouse monoclonal anti-FLAG M2 antibody (Stratagene), and a mouse monoclonal anti-myc antibody (Invitrogen, R950-25). An anti-p94-C-terminus antibody was elicited using C-NVLEWLQLTMYA, corresponding to the C-terminus of rat p94, conjugated to KLH.

RESULTS

Interaction of autolyzed p94 fragments – The autolysis of p94 was reconstituted *in vitro* by mixing p94:C129S and p94Δ, a splicing variant which lacks IS1 and IS2 (8), in a ratio of 10:1. Previously, it was shown that p94Δ recapitulates the substrate-specificity of p94 and retains autolytic activity toward p94:129S, albeit Ca^{2+}-dependently (8). The condition used here allows the detection of the autolyzed fragments from p94:C129S generated by "intermolecular autolytic" activity of p94Δ (8).

In SDS-PAGE analysis, a slight mobility shift of p94:C129S was detected after 15 min of incubation in the presence of Ca^{2+} (Fig. 1B, open and closed arrowheads); it is caused by very rapid cleavages at the N-terminus (Fig. 1A, arrows [1]). Subsequently, 55 kDa and additional smaller autolyzed fragments were generated (Fig. 1B, arrows) (16). Since N-terminal cleavages do not impair the proteolytic activity of p94Δ (8), it was assumed that both the full-length and N-terminally clipped populations of p94:C129S (Fig. 1B, open and closed arrowheads, respectively) represent structures of protease-active p94 species.

The same set of samples was analyzed by native-PAGE to examine the change of molecular conformation. After 15 min of incubation, p94:C129S slightly shifted toward the lower end of the gel (Fig. 1C, CS+Δ, lanes 15′ to 240′, open and closed arrowheads). This mobility shift most probably reflects the N-terminal cleavage detected in Fig. 1B (open and closed arrowheads), because incubation of p94:C129S alone did not cause a significant change in mobility or signal intensity (Fig. 1C, CS), and the mobility of p94Δ does not overlap with that of p94:C129S in native-PAGE (Fig. 1C, arrows).

By size-exclusion chromatography, we have previously shown the possibility that purified recombinant p94:C129S forms a homodimer (12). The bands detected by the native-PAGE may correspond to p94:C129S homodimer. It is not likely, however, that the observed mobility shift of p94:C129S is caused by monomer-dimer conversion as the shift is probably too small for the change of molecular mass between 94 kDa (monomer) and 188 kDa (dimer).

The sum of the full-length and N-terminally clipped fragments detected by SDS-PAGE was compared to those detected by native-PAGE by densitometry (Fig. 1D). When the samples were subjected to SDS-PAGE, the rapid decline was observed ($t_{1/2}$ = about 140 min; Fig. 1D, closed circles). In native-PAGE analysis, however, more than 60% of the initial density was maintained for up to 4 hours (Fig. 1D, open circles). Western blot analysis with an anti-pIS2 antibody following SDS- or native-PAGE showed the same trend, *i.e.*, slower decrease of the signal intensity for the full-length and the N-terminally cleaved p94:C129S under non-denaturing condition (Figs. 1B and C, anti-pIS2).

These observations indicate that intermolecular autolytic cleavages of p94 do not simultaneously generate separate autolyzed fragments, and that these fragments maintain their initial intramolecular interaction for more than twice the time predicted by SDS-PAGE analysis. This population of autolyzed p94 might be described as "IS1-nicked" molecules, because the 55 kDa fragment detected in SDS-PAGE (Fig. 1B, the uppermost arrow) corresponds to the C-terminal product generated by autolysis in IS1 (Fig. 1A, arrows [2]).

A cryptic autolytic site of p94 near the N2A connectin binding region – In COS7 cell expression system, the amount of wild type p94 detected as the 55 kDa fragment is considerably smaller than that of the 94 kDa fragment for the protease-inactive p94:C129S mutant (Fig. 2A, WT and CS). This observation indicates that NS and IS1 are dominant, but not the only sites for autolysis, and that wild-type p94 further undergoes autolysis at several unidentified sites.

To reveal other autolytic sites, p94:ex6$^-$, a splice variant that lacks the IS1 region encoded by exon 6 (26), was used. p94:ex6$^-$ is detectable as full-length molecules of the calculated size (89 kDa; Fig. 2A, arrow), and does not undergo autolysis as exhaustively as does wild-type p94 (open arrowhead). This variant undergoes autolytic cleavages in its NS region, and also proteolyzes p94:C129S to generate the 55 kDa fragment (data not shown). Therefore, it is suggested that p94:ex6$^-$ retains an autolytic profile similar to wild-type p94 except for altered autolysis of itself in IS1. An autolytic fragment of *ca.* 32 kDa (Fig. 2A, closed arrowhead) was abundantly detected for p94:ex6$^-$ by anti-pIS2 antibody. This indicates

the existence of another cryptic autolytic site in the C-terminal half of p94. Very small or no amount of the 32 kDa fragment was detected in wild type p94 or the C129S mutant, respectively.

To detect autolytic cleavage in the C-terminal region of p94 more efficiently, wild-type p94 and p94:ex6$^-$ with C-terminal myc and 6×His epitope tags (together causing an increase of about 3 kDa) were expressed in COS7 cells and immunoprecipitated using anti-pIS2 (data not shown) or anti-myc antibodies (Fig. 2B). The 55 kDa autolyzed fragment of wild-type p94 was detected as a 58 kDa C-terminal fragment for myc-His-tagged wild-type p94, consistent with the calculated +3 kDa size (Fig. 2B, open arrowhead). Smaller fragments of *ca.* 35 kDa, was detected for p94:WT- and p94:ex6$^-$-myc-His, but not for protease-inactive p94:ex6$^-$:C129S-myc-His (Fig. 2B, closed arrowhead). Since the 35 kDa bands contain a myc C-terminal epitope, the proteolytic site for these autolyzed fragments was predicted to be the N-terminus of the IS2 region of p94 (Fig. 1A, arrow [3]).

Analysis of intramolecular autolysis using the p94:N358D mutant – To understand further the autolytic processes of p94, autolysis was examined using an active site mutant, p94:N358D. The substitution of active site Asn to Asp was reported to result in very low, but not zero, specific activity by affecting the interaction between active site residues (28). Similarly, p94:N358D showed weakened autolytic activity, unlike p94:C129S whose activity is zero. Partially purified recombinant p94:N358D protein was incubated at 37°C, and the generation of several different autolytic fragments was detected by a panel of anti-p94 antibodies (Figs. 1A and 2C). Based on the molecular size as well as the reactivity to each antibody, the major autolytic fragments were categorized into three groups, labeled as a, b, and c (Fig. 1A, bidirectional arrows; Fig. 2C, open arrowheads). During the first 5 min of autolysis, generation of fragments "a" and "b", as initially 35 kDa and 58 kDa bands, respectively, were detected (Fig. 2C, arrowheads a and b), and, concomitantly, most of the full-length protein disappeared (Fig. 2C, black arrowhead). The fragments "a" retained reactivity to anti-pNS antibody, indicating that the autolysis in IS1 occurs very fast, whereas that in NS does not. In the late phase of autolysis, several bands of around 32 kDa (Fig. 2C, c) were faintly detected by the anti-pIS2 antibody. The fragment sizes suggest that at least one of these bands corresponds to the C-terminal autolytic fragment generated by a cut in the proximity of IS2 as identified above. Although the identical band should be detected by the anti-C-terminal antibody, the titer of the anti-C-terminal antibody, about 1/100 that of anti-pIS2, fell short of the detection limit.

Presuming that p94:N358D has weak otherwise normal autolytic/protease activity, this mutant illustrates the proceeding of intramolecular autolysis of p94, *i.e.*, cuts in IS1 occur very rapidly, followed by a relatively slow cut in IS2, whereas a cut in NS does not happen significantly under the conditions used. These features are in contrast to those in intermolecular autolysis, *i.e.*, between active p94 variants, such as p94Δ and p94:ex6$^-$, and protease inactive p94:C129S, where NS proteolysis happens first, indicating that NS is prone to being cut intermolecularly by other p94 molecules rather than intramolecularly.

In both cases, a cut in IS2 is likely to disassemble the p94 molecule. After the cut in IS2, the N-terminal part, domain II + III with nicks in IS1, may retain the structure for proteolytic activity until it is subjected to further proteolysis.

Establishment of an assay system for p94 autolytic activity using fusion proteins with Gal4 functional domains – As an approach to assessing the autolytic processes of p94 semiquantitatively, the yeast transcriptional activator Gal4 system was modified according to a previous study on autolytic processing of 3C protease (24). Transcriptional activation by Gal4 requires that its two functional domains, Gal4bd (BD) and Gal4ad (AD), stay proximal to each other. Those domains are linked by p94 to be expressed as a BD–p94–AD hybrid protein. A hybrid protein containing wild-type p94 (BD–p94:WT–AD) is anticipated to fail to activate reporter genes, as BD and AD become separated from each other upon p94 autolysis, especially in IS2, as discussed above (Fig. 3A, upper). In contrast, a hybrid protein composed of protease-inactive p94:C129S mutant (BD–p94:C129S–AD) remains as the full-length fusion protein, and, therefore, is expected to be capable of activating transcription (Fig. 3A, lower).

Using the *S. cerevisiae* AH109 and CG1945 strains as hosts, transcriptional activation of the reporter genes *HIS3*, *ADE2*, and *LacZ* by BD–p94–AD hybrid proteins was examined. As expected, transformants expressing the hybrid protein for p94:C129S but not for wild-type p94 were able to grow on plates without His and Ade, *i.e.*, expression of *HIS3* and *ADE2* was activated (Fig. 3B, SD–WHA). Liquid culture assays for β-galactosidase activity, an index for reporter gene, *LacZ*, expression, gave an essentially identical result: 12.9 ± 3.7 units for WT and 770 ± 175 units for C129S.

Coexpression of intact wild-type p94 with BD–p94:C129S–AD resulted in a slight reduction, but not a complete loss, of the reporter gene expression by BD–p94:C129S–AD (data not shown). Since the viability of yeast cells expressing BD–p94:WT–AD on SD–W plates is comparable to that expressing BD–p94:C129S–AD (Fig. 3B, SD–W), it is not likely that the protease activity of p94 against yeast proteins is a dominant factor causing the phenotypes observed above, unlike poliovirus protease 2A (23). Together, it was concluded that rapid autolysis of p94 causes the dissociation of BD and AD, and is detected as the lack of reporter gene expression in yeast cells.

Detection of altered autolytic activity by point mutations – To test the applicability of Gal4–p94 hybrid constructs for semiquantitative analysis of p94 autolysis, point mutations in domain III, R490W and R572Q, were introduced to the BD–p94:WT–AD fusion protein. These mutations were originally identified as pathogenic missense mutations of p94 found in LGMD2A patients, and both mutant p94s undergo autolysis but not as exhaustively as wild-type p94 does when expressed in COS7 cells (6).

The yeast cells expressing BD–p94:R490W–AD were able to grow on plates that lack His and Ade, however, more slowly than those expressing BD–p94:C129S–AD (Fig. 3B, SD–WHA, 2day and 3day). Therefore, it is suggested that reduced autolytic activity of R490W mutant allowed the expression of reporter genes, *HIS3* and *ADE2*, albeit less efficiently compared to C129S mutant. The same trend was observed for BD–p94:R572Q–AD (data not shown).

To compare the activity of the hybrid proteins with different mutations more quantitatively, liquid culture assay for β-galactosidase activity was performed. Under the conditions where the measured value for p94:C129S remained within the linear range, the following values were obtained; 1.64 ± 0.48, 172 ± 26, 60.7 ± 18, and 30.0 ± 1.8 units for WT, C129S, R490W, and R572Q, respectively. The results were presented relative to the activity of BD–p94:C129S–AD, which was set to 100 (Fig. 3C). Transcriptional activation by the hybrid BD–p94–AD with R490W or R572Q mutation was significantly more efficient than that by BD–p94:WT–AD ($P < 0.001$, $n = 4$), but was not as strong as that by BD–p94:C129S–AD. Together, it was shown that reduced autolytic activity by the mutations R490W and R572Q can be recapitulated as an increased efficiency in transcriptional activation by hybrid proteins with those mutations.

In summary, the presented system is competent to assay the autolytic activity of p94 by assessing the deceleration of the autolysis of p94. Evaluation of the accelerating effects on p94 autolytic activity was difficult as the value for wild-type hybrid proteins was close to the lower end of the measurable range for liquid culture assays.

Screening of mutations that inactivate p94 – One of important application of the above system could be to study structure-function relationships regarding p94 autolytic activity. The applicability was tested by screening of p94 mutants with reduced autolytic activity. Random mutations were introduced into domain II of the BD–p94:WT–AD hybrid protein by PCR and *in vivo* homologous recombination, and the mutations that allowed the expression of reporter genes, *HIS3* and *ADE2*, were identified (Fig. 4A).

About 2×10^6 transformed colonies were screened on selection medium plates, SD–WHA, resulting in about 3,400 grown colonies. Among them, 276 colonies were picked, and plasmid DNAs were rescued from 23 colonies. Each plasmid encoded the BD–p94–AD hybrid protein with up to 5 missense mutations in a region of about 300 amino acid residues, corresponding mainly to domain II (Table 1 and Fig. 4B).

It should be noted that among the 34 missense mutations identified in 23 clones, (i) a W369R mutation, where W369 is a highly conserved residue in the calpain family (3), was found in 10 clones; and (ii) six loci, T184, R386, G329, Y336,

G367, and N449, were where missense mutations are found in LGMD2A patients, among which four substitutions, T184M, R386C, G329R, and G367S were exactly identified in LGMD2A patients (29).

For each clone, most probable mutation(s) responsible for inactivating p94 was(were) deduced considering the extent how well the residue is conserved and/or whether the identical mutation is found in LGMD2A patients (Table 1). Five mutations, Q123H, W376C, W369R, W365R, and L387P, are not included in the 133 pathogenic LGMD2A missense mutations reported so far, and were considered to be responsible for inactivation of p94 in our random mutagenesis experiments. These results indicate that our system is adequate for revealing critical amino acid residues for p94 activity, with large scale-screening planned in the future.

Effect of connectin–p94 interactions during the p94 autolytic process – Two distinct regions of connectin, N2A and the C-terminus, have been identified as binding sites for p94 in the sarcomere (16) (Fig. 5A, CN48 and CN52). These fragments were coexpressed in yeast cells with BD–p94–AD to test whether or not autolytic activity of p94 is affected by the interaction with connectin. The rationale was that a partial, if not the complete, interference in the autolytic process of p94 could yield detectable expression of reporter genes if the presence of a hybrid protein over a certain threshold amount was achieved.

Expression of BD–p94:WT–AD in yeast cells transformed with the empty vector resulted in the lack of growth on SD-LWHA, which is identical to and consistent with the result shown in Fig. 3B (Fig. 5B, SD–LWHA, BD–WT–AD + mock). Coexpression of CN48, but not CN52, restored transcriptional activation of reporter genes, *HIS3* and *ADE2*, by BD–p94:WT–AD as shown by growth on SD–LWHA plates (Fig. 5B, SD–LWHA, BD–WT–AD + CN48 or CN52). Yeast cells expressing the protease-inactive hybrid, BD–p94:C129S–AD, which is by itself functional as a transcriptional activator (Fig. 3B and 3C), was able to grow on a SD–LWHA plate independently of coexpressed connectin fragments (Fig. 5B, SD–LWHA, BD–C129S–AD). The protease-inactive hybrid without the C-terminal AD domain, was not capable of activating transcription (Fig. 5B, SD–LWHA, BD–C129S).

Detailed mapping of the N2A connectin binding region in p94 by conventional yeast two-hybrid assay revealed that the region between V573 and L580, just upstream of the IS2 region, is required for interaction with N2A connectin (Fig. 1A). This region coincides with the cryptic autolytic site identified above, which is predicted to be critical for autolytic disassembly of the p94 molecule.

Together, these data indicate that the CN48 connectin fragment, which binds to p94, is able to retain BD and AD of the hybrid protein proximal to each other, against the p94 autolytic activity. This is the first demonstration that shows suppressive effect of N2A connectin on autolytic disassembly of p94, presenting the biological significance of p94–N2A connectin interaction.

A mutant connectin fragment corresponding to the mdm deletion was not able to bind p94 or stabilize p94 – The mouse N2A connectin fragment (denoted as mCN48) with pathogenic mutation (*mdm*) was examined as to its effect on p94 autolysis. Recessively inherited mouse muscular dystrophy, *mdm*, is caused by an 83-aa deletion in N2A connectin (18,30). In the conventional yeast two-hybrid system, the *mdm* deletion abolished the p94-connectin interaction as we previously reported (Fig. 5A, mCN48–mdm, (20)). Coexpression of mCN48–mdm with Gal4–p94 hybrid protein failed to restore transcriptional activation of reporter genes by BD–p94:WT–AD, but did not interfere with transcriptional activation by BD–p94:C129S–AD (Fig. 5C, SD–LWHA). This shows that the pathogenic *mdm* deletion abolished N2A connectin's ability to regulate autolytic process of p94, which indicates further impairment in p94 functions under *mdm* conditions.

DISCUSSION

In this study, the interaction between the autolyzed fragments of p94 and the effects of the connectin–p94 interaction during autolysis were analyzed. Using the *in vitro* reconstituted autolytic reaction of full-length p94, it was suggested that p94 retains functional conformation as a protease during autolysis. Furthermore, we have developed a genetic method of studying the autolytic properties of p94. The validity of the system for detecting changes in p94 autolytic activity and

examining the effects of interacting molecules, particularly connectin/titin fragments, in autolytic process has been demonstrated. These data provide a model for a molecular mechanism how connectin is involved in the regulation of p94.

It has been anticipated that p94 autolysis would result in disruption of the protease core, *i.e.*, in inactivation of p94, as dominant autolytic sites of p94 resides in the IS1 region between the active site Cys129 and His334/Asn358 (Fig. 1A, arrows [2]). Thus, the amount of active p94 was expected to be quickly reduced during autolysis. Nevertheless, several proteins besides p94 itself were substantially proteolyzed in COS7 cells expressing p94 (6), casting a doubt about the assumption that autolysis of p94 immediately inactivates p94.

Several different approaches using fragments of p94 argue for the association of autolyzed fragments of p94 (10,31). The protease core of p94, corresponding to the region NS–IIa–IS1–IIb (Fig. 1A upper panel), undergoes Ca^{2+}-dependent autolytic processing in the NS and IS1 regions. The cleavages in NS and IS1 were demonstrated to precede the gain in protease activity against other substrate molecules, and the interaction between autolyzed fragments was biochemically shown (10). These reports, however, have not shown information about the whole structure of p94.

In this study, association of autolyzed fragments shown by native-PAGE analysis, in which p94:C129S was intermolecularly autolyzed by p94Δ, clearly indicates that not only the protease core but also almost whole structure of p94 retain its intact conformation for some time after autolysis. Therefore, these results including ours indicate that p94 expresses its protease activity even with nicks in IS1 by autolysis, which answers the question of why endogenous proteins such as HSP60 and calpastatin were properly proteolyzed regardless of full-length p94 being hardly detected when expressed in COS7 cells (6).

Furthermore, another autolytic site in p94 was identified at the N-terminus of IS2. This may explain the fact that the 55 kDa autolytic fragment corresponding to the structure from IS1 to the C-terminus is detected much less than expected. Lp82, a lens-specific splicing variant of p94, was reported to have an autolytic site between domains III and IV corresponding to the N-terminus of R592 of p94 (11), which is probably identical to the autolytic site revealed in this study. The data suggests that IS2, which has been considered to play a role for modulating the Ca^{2+}-dependence of p94 (32,33), is also involved in the autolysis together with NS and IS1.

Autolytic reaction reconstituted using p94:C129S and p94Δ as substrate and active enzyme, respectively, proceeds too rapidly to capture the sequential involvement of NS, IS1, and IS2 in the process. Therefore, another p94 mutant, p94:N358D was used for comparing the generation of different autolytic fragments using much lower concentration of p94 protein ($[p94:N358D]^2$ is *ca.* 1/1,000 of [p94:C129S][p94Δ], as their concentrations are 0.01, 1, and 0.1 mg/ml, respectively) to make the intramolecular autolysis predominant. It has been shown that the m-calpain:N286D mutant has very weak activity determined by caseinolytic assay; the weak protease activity is because of the impairment of the interaction between active site residues rather than the alteration in Ca^{2+}-sensitivity (28). Native p94 partially purified from rabbit skeletal muscle first autolyzes at the N-terminus of G275 in IS1, yielding *ca.* 60 kDa fragments, which eventually converges to a 55 kDa fragment by a further cut in the N-terminus of E323 (12). The autolytic profile of p94:N358D essentially reproduced the trend (Fig. 2C, anti-pIS2), supporting the idea that this mutant has weak but otherwise unaltered autolytic activity, and, therefore, is appropriate for the experiment here.

It has been observed that autolysis in the NS region is very rapid in intermolecular reactions but is relatively slow in intramolecular reactions; the ratio of both reactions depends on the concentrations of p94. This would explain why the *in vitro* autolysis of p94:C129S by p94Δ showed quick NS proteolysis (Fig. 1B), whereas the autolysis of lower concentrated p94:N358D did not (Fig. 2C). It is, however, the cleavage in IS1 that is observed in the early phase of autolysis in both cases. The small C-terminal autolyzed fragment cut in the proximity of IS2 is generated later. Therefore, it was concluded that a cut in IS2 is slow but critical for disassembly of autolyzed p94 fragments. As summarized in Fig. 6A, the speculated procedure of autolytic cleavage is, intermolecularly, the order of proteolysis is NS (b) → IS1(c) → IS2(d), and intramolecularly, it is IS1(e) → IS2(f) → NS.

As an approach complementary to *in vitro* study of p94 autolysis described above, we have established a system for monitoring p94 autolytic activity using a Gal4-based transcriptional activation system. Developing such a system was expected to make it feasible to capture the behavior of p94 by evaluating its autolysis and then to screen mutations/factors influencing p94 autolytic activity. Experiments using LGMD2A mutants clearly showed that the system is competent for detecting changes in p94 autolytic activity semiquantitatively. Furthermore, using this system for screening as performed here has following advantages: (i) non-sense mutations, which terminate polypeptide chain somewhere in p94, *i.e.*, between BD and AD, are intrinsically eliminated; and (ii) specific domains can be selected to introduce mutations for structure–functional studies. These features greatly improve the efficiency of identification and characterization of the mutants, which can be applied to primary, if not decisive, diagnosis for LGMD2A. One of the significant applications of the system would be screening of conditionally inactive mutants of p94, *e.g.*, temperature-sensitive mutants of p94 that could be beneficial for protein expression and purification.

The BD–p94:WT–AD hybrid protein caused no detectable transcription of the reporter genes, indicating that autolysis is fast enough to result in a state where the major parts of BD and AD are dissociated. Based on the scheme for autolytic process of p94 in Fig. 6A, there are two possibilities that can dissociate BD from AD; a cut in NS to liberate N-terminally fused BD, and/or a cut in IS2 to dissociate the C-terminal fragment of p94 fused to AD. The former and the latter, respectively, happen preferentially in inter- and intra-molecular autolyses (Fig. 6A, (b) and (f)). Coexpression of BD–p94:C129S–AD and p94:WT reduced the reporter gene activation to some extent, but not to zero, indicating that the intramolecular reactions predominates over the intermolecular reactions in yeast cells, and/or that NS became less accessible because of the fusion with BD. In both cases, the IS2 cut is more likely to casuse BD/AD dissociateion. Although the *in vitro* analyses suggest that autolysis in IS2 occurs relatively slowly after that in IS1, our results indicate that autolysis in IS2 of BD–p94:WT–AD is fast enough not to provoke reporter gene expression in yeast.

The above hybrid protein assay in yeast clearly demonstrated for the first time that N2A connectin, encoded by the clone CN48, interacts directly with p94 to suppress autolytic process of p94. The molecular mechanisms of how N2A connectin affects p94 autolysis could be inferred as "suppression" rather than "inhibition" of autolysis, as coexpression of the CN48 fragment with p94 in cultured cells did not significantly inhibit the p94 autolysis (12). Considering that N2A connectin binding site in p94 is in the vicinity of the autolytic site proximal to IS2, presumably between D591 and R592, N2A connectin is likely to affect the autolysis in this site by structural hindrance (Fig. 1A and Fig. 6A (g)). It is unlikely that the above autolysis disrupts connectin binding sequence in p94, because the p94:S581term mutant, which does not have a C-terminal part after S581, can bind N2A connectin (Fig. 1A).

Alternatively, weak interactions between CN48 and IS2/domain IV that could not have been detected by the conventional yeast two-hybrid system may delay the complete dissociation of BD and AD, even after a cut in/near IS2 (Fig. 6A (h)).

In contrast, the interaction between p94 and the C-terminus of connectin (CN52) detected in the conventional yeast two-hybrid system (15,16) failed to be evaluated in the hybrid protein assay. As CN52 requires full-length p94 structure (15), CN52 also must suppress autolysis in IS2. If p94:WT were autolyzed at IS2, it would cause dissociation of the C-terminal part, resulting in inability in binding CN52. A possible account for this apparent discrepancy is that the full-length p94 structure, which is required for CN52 binding (15), might be compromised by simultaneous addition of BD and Ad. The alternative approach is required for determining the biological significance of p94–connectin C-terminus interaction.

An in-frame deletion of mouse N2A connectin has been shown to cause severe muscular dytrsophy, *mdm*, and the binding of CN48 to p94 was suggested to be disrupted by this mutation (Fig. 5A) (18,20). In this study, one of the physiological consequences of such a deletion was suggested to be the lack of regulation of p94 autolysis, which can explain decreased p94 protein levels in *mdm* homozygous skeletal muscle reported by several studies (18,19,34).

The relationship between the activity of p94 and *mdm* pathology has been studied using mutant mice that have the connectin *mdm* mutation combined with p94 gene knockout or overexpression of wild-type p94 (34). Transgenic overexpression of p94 in *mdm* homozygous ($Ttn^{mdm/mdm}$) mice caused exacerbation of the dystrophic phenotype (34), while it yields almost no phenotype in wild type mice (35). Moreover, gait activity is slightly altered in *mdm* heterozygous ($Ttn^{+/mdm}$) mice, and transgenic overexpression of wild-type p94 corrected this feature. Together with the results presented in this study and the fact that N2A connectin is present in stoichiometric excess over p94 in skeletal muscle, these phenotypes can be explained as follows: p94 overexpression (i) shows no toxicity in wild-type mice, because N2A connectin absorbs excess p94 and suppresses p94 activity; (ii) was detrimental in $Ttn^{mdm/mdm}$ mice, because free p94, which cannot be absorbed due to the *mdm* mutation, attacks myofibril proteins; and (iii) corrected mild phenotypes in $Ttn^{+/mdm}$ mice, because a sufficient amount of p94 was supplied to cancel the imbalance between molecular components at the N2A region; *e.g.*, in *mdm* homozygous skeletal muscle, another binding protein in N2A region of connectin, CARP (cardiac ankyrin-repeat protein)/MARP1 (muscle ankyrin-repeat protein 1) is upregulated (20). These highlight the functional crosstalk between p94 and other muscle proteins in the N2A region.

The minimum p94-binding region in N2A connectin corresponds to two tandem IG domains, denoted as I82 and I83, at the C-terminus of N2A (20). As shown in Fig. 6B, *mdm* deletion causes truncation of the last two β-strands of the C-terminal IG domain (I83); the 3D structure of I82–I83 in Fig. 6B is deduced from the reported structure of Z1–Z2, other IG repeat modules in the connectin molecule. The deletion may destroy the structure of I83 necessary for binding and stabilizing p94.

It should be noted that the p94-binding region region is in the vicinity of the so-called PEVK region, rich in Pro, Glu, Val, and Lys, and composed of random coils. The PEVK region has been considered to play a key role in expressing passive elasticity. This region is recently described as “intrinsically unstructured protein (IUP)” (36), and is similar to another IUP, calpastatin, an endogenous inhibitor protein for the conventional calpains. Besides the direct suppressive effect of N2A connectin on p94 autolytic disassembly, it is possible that the adjacent PEVK region is positioned so that it modulates p94 activity, for example, by serving as a pseudosubstrate, because calpastatin has been identified as one of the best substrates for p94 so far (8).

Our hybrid protein assay demonstrated the suppressive effect of N2A connectin on p94 autolysis; however, it seems that additional cellular components, which could be specific to skeletal muscle cells, are required for maintaining the full-length p94 protein at an amount sufficient for its function. Immunodetection shows that considerable amounts of the full-length p94 protein exist as the major molecular species in skeletal muscle tissue ((13), Ojima *et al.*, unpublished results). Furthermore, the autolytic properties of p94 are probably relevant under those cellular context for maintaining the proper amounts of its activity. For example, unlike wild-type p94, overexpression of one of the splice variants of p94 lacking IS1, p94:ex6$^-$, which is rather resistant to autolytic degradation, interfered with normal muscle maturation (35). In addition to directly interacting molecules, it is possible that there are factors that potentiate the proper amount of p94 activity, *e.g.*, through changing the local Ca^{2+} concentrations or regulation of the expression spectra of p94 splice variants. Further studies are required for complete elucidation of the regulation of p94 activity, which will lead to an understanding of the true roles of p94 in skeletal muscle and its involvement in muscular dystrophy when defective.

REFERENCES

1. Suzuki, K., Hata, S., Kawabata, Y., and Sorimachi, H. (2004) *Diabetes* **53**, S12-18
2. Goll, D. E., Thompson, V. F., Li, H., Wei, W., and Cong, J. (2003) *Physiol Rev* **83**, 731-801
3. Sorimachi, H., and Suzuki, K. (2001) *J Biochem* **129**, 653-664
4. Sorimachi, H., Imajoh-Ohmi, S., Emori, Y., Kawasaki, H., Ohno, S., Minami, Y., and Suzuki, K. (1989) *J Biol Chem* **264**, 20106-20111
5. Richard, I., Broux, O., Allamand, V., Fougerousse, F., Chiannilkulchai, N., Bourg, N., Brenguier, L., Devaud, C., Pasturaud, P., Roudaut, C., and et al. (1995) *Cell* **81**, 27-40
6. Ono, Y., Shimada, H., Sorimachi, H., Richard, I., Saido, T. C., Beckmann, J. S., Ishiura, S., and Suzuki, K. (1998) *J Biol Chem* **273**, 17073-17078
7. Sorimachi, H., Toyama-Sorimachi, N., Saido, T. C., Kawasaki, H., Sugita, H., Miyasaka, M., Arahata, K., Ishiura, S., and Suzuki, K. (1993) *J Biol Chem* **268**, 10593-10605
8. Ono, Y., Kakinuma, K., Torii, F., Irie, A., Nakagawa, K., Labeit, S., Abe, K., Suzuki, K., and Sorimachi, H. (2004) *J Biol Chem* **279**, 2761-2771
9. Rey, M. A., and Davies, P. L. (2002) *FEBS Lett* **532**, 401-406
10. Diaz, B. G., Moldoveanu, T., Kuiper, M. J., Campbell, R. L., and Davies, P. L. (2004) *J Biol Chem* **279**, 27656-27666
11. Fukiage, C., Nakajima, E., Ma, H., Azuma, M., and Shearer, T. R. (2002) *J Biol Chem* **277**, 20678-20685
12. Kinbara, K., Ishiura, S., Tomioka, S., Sorimachi, H., Jeong, S. Y., Amano, S., Kawasaki, H., Kolmerer, B., Kimura, S., Labeit, S., and Suzuki, K. (1998) *Biochem J* **335 (Pt 3)**, 589-596
13. Kramerova, I., Kudryashova, E., Tidball, J. G., and Spencer, M. J. (2004) *Hum Mol Genet* **13**, 1373-1388
14. Anderson, L. V., Davison, K., Moss, J. A., Richard, I., Fardeau, M., Tome, F. M., Hubner, C., Lasa, A., Colomer, J., and Beckmann, J. S. (1998) *Am J Pathol* **153**, 1169-1179
15. Kinbara, K., Sorimachi, H., Ishiura, S., and Suzuki, K. (1997) *Arch Biochem Biophys* **342**, 99-107
16. Sorimachi, H., Kinbara, K., Kimura, S., Takahashi, M., Ishiura, S., Sasagawa, N., Sorimachi, N., Shimada, H., Tagawa, K., Maruyama, K., and Suzuki, K. (1995) *J Biol Chem* **270**, 31158-31162
17. Keira, Y., Noguchi, S., Minami, N., Hayashi, Y. K., and Nishino, I. (2003) *J Biochem* **133**, 659-664
18. Garvey, S. M., Rajan, C., Lerner, A. P., Frankel, W. N., and Cox, G. A. (2002) *Genomics* **79**, 146-149
19. Haravuori, H., Vihola, A., Straub, V., Auranen, M., Richard, I., Marchand, S., Voit, T., Labeit, S., Somer, H., Peltonen, L., Beckmann, J. S., and Udd, B. (2001) *Neurology* **56**, 869-877
20. Witt, C. C., Ono, Y., Puschmann, E., McNabb, M., Wu, Y., Gotthardt, M., Witt, S. H., Haak, M., Labeit, D., Gregorio, C. C., Sorimachi, H., Granzier, H., and Labeit, S. (2004) *J Mol Biol* **336**, 145-154
21. Liebig, H. D., Skern, T., Luderer, M., Sommergruber, W., Blaas, D., and Kuechler, E. (1991) *Proc Natl Acad Sci U S A* **88**, 5979-5983

22. Dautin, N., Karimova, G., Ullmann, A., and Ladant, D. (2000) *J Bacteriol* **182**, 7060-7066
23. Barco, A., Ventoso, I., and Carrasco, L. (1997) *J Biol Chem* **272**, 12683-12691
24. Dasmahapatra, B., DiDomenico, B., Dwyer, S., Ma, J., Sadowski, I., and Schwartz, J. (1992) *Proc Natl Acad Sci U S A* **89**, 4159-4162
25. Sato, N., Kawahara, H., Toh-e, A., and Maeda, T. (2003) *Mol Cell Biol* **23**, 6662-6671
26. Herasse, M., Ono, Y., Fougerousse, F., Kimura, E., Stockholm, D., Beley, C., Montarras, D., Pinset, C., Sorimachi, H., Suzuki, K., Beckmann, J. S., and Richard, I. (1999) *Mol Cell Biol* **19**, 4047-4055
27. Longtine, M. S., McKenzie, A., 3rd, Demarini, D. J., Shah, N. G., Wach, A., Brachat, A., Philippsen, P., and Pringle, J. R. (1998) *Yeast* **14**, 953-961
28. Arthur, J. S., Gauthier, S., and Elce, J. S. (1995) *FEBS Lett* **368**, 397-400
29. Richard, I., Roudaut, C., Saenz, A., Pogue, R., Grimbergen, J. E., Anderson, L. V., Beley, C., Cobo, A. M., de Diego, C., Eymard, B., Gallano, P., Ginjaar, H. B., Lasa, A., Pollitt, C., Topaloglu, H., Urtizberea, J. A., de Visser, M., van der Kooi, A., Bushby, K., Bakker, E., Lopez de Munain, A., Fardeau, M., and Beckmann, J. S. (1999) *Am J Hum Genet* **64**, 1524-1540
30. Muller-Seitz, M., Kaupmann, K., Labeit, S., and Jockusch, H. (1993) *Genomics* **18**, 559-561
31. Taveau, M., Bourg, N., Sillon, G., Roudaut, C., Bartoli, M., and Richard, I. (2003) *Mol Cell Biol* **23**, 9127-9135
32. Shih, M., Ma, H., Nakajima, E., David, L. L., Azuma, M., and Shearer, T. R. (2005) *Exp Eye Res* **82**, 146-152
33. Ma, H., Shih, M., Fukiage, C., Azuma, M., Duncan, M. K., Reed, N. A., Richard, I., Beckmann, J. S., and Shearer, T. R. (2000) *Invest Ophthalmol Vis Sci* **41**, 4232-4239
34. Huebsch, K. A., Kudryashova, E., Wooley, C. M., Sher, R. B., Seburn, K. L., Spencer, M. J., and Cox, G. A. (2005) *Hum Mol Genet* **14**, 2801-2811
35. Spencer, M. J., Guyon, J. R., Sorimachi, H., Potts, A., Richard, I., Herasse, M., Chamberlain, J., Dalkilic, I., Kunkel, L. M., and Beckmann, J. S. (2002) *Proc Natl Acad Sci U S A* **99**, 8874-8879
36. Tompa, P. (2002) *Trends Biochem Sci* **27**, 527-533

FOOTNOTES

* We are grateful to all of our laboratory members for experimental support and valuable discussion. This work was supported in part by MEXT.KAKENHI 16026209 (to HS), and 14656054 (to KA), by JSPS.KAKENHI 15380089 (to HS), KAKENHI 14086203 (to TM), a grant (No.0349) from the Salt Science Research Foundation (to TM), a grant from DFG (La 1969/1-1, to DL), and a Research Grant (17A–10) for Nervous and Mental Disorders from the Ministry of Health, Labor and Welfare (to HS).

The abbreviations used are: LGMD2A, limb-girdle muscular dystrophy type 2A; NS, N-terminal sequence unique to p94; IS1 (IS2), insertion sequence 1 (2) unique to p94; CN48 (CN52), connectin/titin clone No. 48 (52); AD, activation domain of Gal4; BD, DNA binding domain of Gal4; CARP (MARP), cardiac (muscle) ankyrin repeat protein; *mdm*, muscular dystrophy with myositis; PEVK, flexible region of connectin rich in Pro, Glu, Val, and Lys; SD–W etc., synthetic minimal medium with dextrose minus tryptophan etc.

FIGURE LEGENDS

Fig. 1. Connectin binding and autolytic profiles of p94.
A, Upper panel; A schematic of the molecular structure of p94. NS, IS1, and IS2 are p94-specific insertion sequences. Subdomains IIa and IIb compose the calpain protease domain. Domains III and IV are C2-like Ca^{2+}-binding and 5EF-hand motif domains, respectively. Arrows [1] to [3] indicate proteolytic sites for autolysis. The positions of the epitopes for the antibodies used in this study and the deduced positions of the fragments indicated by open arrowheads in Fig. 2C (a–c) are shown by the bracketed lines and the bidirectional arrows, respectively. The bars under the schematic structure represent the result from yeast two-hybrid assay for surveying the sites in p94 required for interaction with N2A connectin. A series of C-terminal truncations (bars) were introduced into p94, and their effect on the binding activity to N2A connectin, clone CN48, was evaluated. Deletion of most of IS2 did not compromise the connectin-binding activity of p94.
B, The autolytic profile of p94:C129S. The intermolecular autolytic reaction was reconstituted *in vitro* using p94:C129S as a substrate for p94Δ. The reaction was stopped at each indicated time and analyzed by SDS–PAGE followed by CBB-staining or immunoblotting using anti-pIS2 antibody. Open and closed arrowheads suggest the full-length and N-terminally clipped molecules, respectively. Arrows indicate the autolyzed fragments of p94:C129S by further proteolysis in IS1 and other regions. A grey arrowhead incicates p94Δ.
C, Native-PAGE analysis of the set of samples shown in B. As controls, p94:C129S, after 240 min incubation with and without Ca^{2+}, and p94Δ were electrophoresed separately. Open and closed arrowheads indicate the mobility corresponding to the full-length and the N-terminally clipped fragments of p94:C129S. The mobility of those two populations is compared at the right side of the panel. Note that the mobility of p94Δ does not overlap with either (arrow).
D, Changes in the sum of the full-length and the N-terminally autolyzed fragments. Signal intensity corresponding to the full-length and the N-terminally autolyzed fragments (open and closed arrowheads in Fig. 1B and C) was measured and plotted against incubation time. The values are standardized with the value at 0 min set to 1. Closed and open circles indicate the values obtained for SDS–PAGE and native-PAGE analysis, respectively.

Fig. 2. Autolysis in the vicinity of the IS2 region
A, Comparison of autolytic fragments. Wild-type p94 (WT), a splice variant that lacks the exon 6-encoded IS1 region (p94:ex6$^-$), and p94:C129S (CS) expressed in COS7 cells were compared by western blotting using an anti-pIS2 antibody. Wild-type p94 is mainly detected as the autolyzed 55 kDa fragment (open arrowhead). For p94:ex6$^-$, the full-length product (arrow) is detected along with autolyzed fragments, in which the 32 kDa fragment is dominant (closed arrowhead).
B, Detection of C-terminal autolyzed fragments. Myc epitope and tandem His hexamer sequences were introduced to the C-terminus of wild-type p94 and p94:ex6$^-$. Constructs were expressed in COS7 cells and immunoprecipitated with an anti-myc antibody. The calculated molecular weight increase caused by the added epitope sequences is about 3 kDa. An autolyzed fragment of calculated molecular size corresponding to 32 kDa in Fig. 2A was recovered for both wild-type p94 and p94:ex6$^-$ (closed arrowhead). The 55 kDa autolyzed fragment generated by proteolysis in IS1 was detected as an approximately 58 kDa fragment only for wild-type p94 with the C-terminal epitope sequence (open arrowhead). Asterisks indicate degradation products unrelated to autolysis. An arrow points the full-length molecule of p94:ex6$^-$ with the C-terminal tag.
C, Analysis of the autolytic processes of p94 by p94:N358D. The active site Asn358 to Asp mutant, p94:N358D, was incubated at 37°C for the indicated times (min). Autolysis of p94 was detected by western blotting using anti-pNS, anti-dIII, anti-pIS2, or anti-C-term antibodies against p94 as indicated. The locations of the fragments marked by the open arrows (a–c) are indicated by the bidirectional arrows in Fig. 1A, upper panel. Fragments a, b, and c correspond to the regions, from the N-terminus to the N-

terminal half of IS2, from the C-terminal half of IS1 to the C-terminus, and from the IS2 to the C-terminus, respectively.

Fig. 3. Autolytic activity of p94 coupled to transcriptional activation by a Gal4–p94 hybrid protein.
A, Schematic overview of transcriptional activation by the Gal4–p94 hybrid protein. Two distinct functional domains of Gal4, the DNA-binding domain (BD) and the transcription-activating domain (AD) were fused to the N-terminus and C-terminus of p94, respectively. A hybrid bearing the wild-type but not the C129S mutant p94 failed to activate transcription because BD and AD are dissociated upon p94 autolysis. Arrows indicate the reported autolytic sites of p94.
B, Growth of yeast AH109 cells transformed with the expression vectors for hybrid proteins. Yeast cells expressing Gal4–p94 hybrid proteins, BD–WT–AD, BD–C129S–AD, or BD–R490W–AD were examined for growth on selection medium. After 2 days on non-selective SD–W plate, expression of those hybrid proteins did not affect the growth of yeast cells. On selective medium without histidine and adenine, SD–WHA, the C129S mutant allowed growth of yeast cells by transcriptional activation of reporter genes, *HI3* and *ADE2*. Yeast cells expressing wild-type hybrid protein did not grow under the same conditions. The R490W mutation caused slow growth of yeast cells, an intermediate phenotype between wild-type and the C129S mutant (compare SD–WHA, 2day and 3day) .
C, Effect of mutations affecting autolytic activity on transcriptional activation by hybrid proteins. Transcriptional activation by a hybrid protein with R490W or R527Q mutations was measured by liquid culture β-galactosidase assay to evaluate the expression of another reporter gene, *lacZ*. Yeast cells expressing C129S produced significant activity. Both R490W and R572Q mutations increased the efficiency of transcription of the reporter gene but did not exceed the efficiency of the C129S mutant. The activity was normalized relative to the value for the C129S mutant protein. $*P < 0.001$ ($n = 4$). Representative results from three independent assays are shown. As expected, there was almost no activity in cells expressing hybrid protein with wild-type p94.

Fig. 4. Screening of p94 mutants defective in autolytic activity.
A, A scheme for screening of mutations that inactivate p94. (a and b) Domain II of the BD–p94:WT–AD hybrid protein was exchanged with domain II fragments harboring random mutation(s). (c) The yeast colonies viable on the selection medium SD–WHA were considered to express hybrid proteins with mutation(s) inactivating p94 autolytic activity. (d) Plasmids for a hybrid protein were rescued from those viable yeast colonies, and the introduced mutations were determined by DNA sequencing.
B, Schematic overview of missense mutations of p94 identified by the screening. The positions of mutations identified by the screening are shown. Based on the definition as described in Table1, the loci are categorized into four (from the upper to the lower); highly conserved in the calpain super family, conserved among p94, μCL, and mCL, conserved among p94, and divergent. *Identical substitutions have been found in LGMD2A patients. **Identical loci have been subjected to point mutations in LGMD2A patients.

Fig. 5. Effect of the connectin–p94 interaction on the autolytic instability of p94.
A, p94 binding regions in connectin. Clones CN48 and CN52 encode the N2A and M-line regions of human connectin, respectively, and they were identified by conventional yeast two-hybrid screening. mCN48 is the same region from mouse connectin. mCN48-mdm has a C-terminal truncation that corresponds to a deletion in connectin produced from the *mdm* allele connectin gene. Bidirectional arrowheads show the relative location in the sarcomere of a connectin molecule. The bracket indicates the region deleted from N2A connectin by the *mdm* mutation. “I” and “M” together with the numbers indicates the IgC2 motif defined in I-band region and M-line region connectin, respectively.
B, Effect of coexpressed connectin CN48 and CN52 fragments. Gal4–p94 hybrid proteins for wild type (BD–WT–AD) or the C129S mutant (BD–C129S–AD), and BD domain fused to the C129S mutant (BD–C129S) or without any fused peptide (BD–), were coexpressed with connectin CN48 or CN52 fragments using yeast expression vector p415GPD (+ CN48 or CN52). As the negative control, coexpression with an

empty vector was included (+ mock). Coexpression with CN48 fragment, but not CN52 fragment, restored transcriptional activity of BD–WT–AD (SD–LWHA, BD–WT–AD). Hybrid constructs of p94:C129S without the C-terminal AD domain (SD–LWHA, BD–C129S) or BD domain alone (SD–LWHA, BD–) showed no transcriptional activity in the presence of either CN48 or CN52. Cells expressing the C129S mutant hybrid protein were capable of grow on selection medium independent of coexpressed fragments (SD–LWHA, BD–C129S–AD). All the combination of coexpression resulted in growth on non-selective medium comparable to each other (SD–LW).
C, Effect of C-terminal truncation in connectin CN48 fragment on p94 hybrid protein activity. Connectin fragments, mCN48 and mCN48-mdm, were expressed using the p425GPD yeast expression vector together with Gal4-p94 hybrid protein as described in B. Coexpression of the mCN48-mdm fragment, which has a C-terminal truncation, with wild type hybrid protein did not result in the growth of yeast cells, suggesting the fragment failed to resotre transcriptional activity of the p94 hybrid protein (SD–LWHA, BD–p94–AD + mCN48-mdm).

Fig. 6. Potential mechanism for N2A connectin binding on p94.
A, A schematic of the autolytic processes of p94. (a) The three arrows and the bidirectional arrow indicate the autolytic sites in the NS, IS1, and IS2 regions and the site for interaction with CN48, respectively. d.II, d.III, and d.IV stand for domains II, III, and IV, respectively. In intermolecular autolysis (*e.g.*, p94:C129S cut by p94Δ), NS is cut very fast (b), followed by cutting of IS1 (c), and finally the molecule dissociates into two after IS2 is cut (d). In intramolecular autolysis (*e.g.*, p94:N358D autolysis at low concentrations), IS1 is cut very fast (e), followed by cutting of IS2 (f), which causes molecular dissociation. If a CN48 fragment exists, suppression of IS2 cutting (g) and/or dissociation after IS2 cutting (h) occurs, resulting in reporter gene expression if the N- and C-terminal ends of the p94 molecule are linked to BD and AD, respectively.
B, Schematic 3D structures of the connectin–p94 interaction. The reported crystal structures of the human m-calpain catalytic subunit (from 1DKV) and Z1–Z2 connectin IG domains (from 1YA5) were aligned in an equal scale to model p94 and I82–I83 IG domains in N2A connectin. The ribbon scheme shown was drawn using MolFeat Ver.2.2 3D imaging software (FiatLux Inc., Tokyo, Japan). The sequence deleted by the *mdm* mutation (indicated in red) composes the last two β-strands of I83 (Z2) structure and extends to the adjacent PEVK region. The spatial size of the two IG domains drawn in this view substantiates their impeditive effect against proteolysis in the IS2 region. Two IG domains are large enough to be an obstacle to proteolysis in the IS2 region.

Table 1. Summary of mutations of p94 harbored in colonies that grew on SD–WHA plates

Bold italic: highly conserved residues in the calpain super family; **Bold**: conserved among p94, μCL, and mCL; *italic*: conserved among human, mouse, chicken, and fugu p94s; "quoted": a residue position where missense mutations are found in LGMD2A patients; underlined: a pathogenic missense mutation found in LGMD2A patients. Most probable responsible mutation(s): estimation is based on the fact that a more widely conserved residue is more crucial for protease activity, *i.e.*, order of precedence is a ***bold italic***, **bold**, and *italic* residue included in the mutations found. If there was more than one residue of the same priority, the underlined residue was chosen.

Mutation(s) identified	Corresponding domain(s)	Most probable responsible mutation(s)	Number of independent clones identified
I121F/W373C[*1]/***D403***V/H407Y[*1]	IIa/IIb × 3	D403V	2
Q123H/***"Y336"***F	IIa/IIb	Q123H[*2]	1
A133T/***G367***S/***S400***Y	IIa/IIb × 2	G367S	1
L140P/*M262*V/***W376***C	IIa/IIb × 2	W376C	1
H151Y/***W369***R	IIa/IIb	W369R	1
T184M/***W369***R	IIa/IIb	T184M and/or W369R	1
S202G/**L387**P	IIa/IIb	S202G and/or L387P	1
*A227*T/M294T[*1]	IIa/IS1	A227T	1
L261P/W373R[*1]/D424V[*1]	IIb × 2/linker	L261P	1
T314P[*1]/*T324*S/***S337***Y/**L387**P	IS1/IIb × 3	S337Y and/or L387P	1
G329R/T339M/**L387**Q	IIb × 3	G329R	1
W365R	IIb	W365R	1
W369R	IIb	W369R	8
S370R/R386C/I405V[*3]/D424G[*1]/***N449***D	IIb × 3/linker/III	R386C[*4]	1
L387P/D424G[*1]	IIb/linker	L387P	1
Total			23

*1: M294, T314, W373, H407, and D424 are divergent residues in the calpain family. M294/T314 and D424 locate, respectively, in the IS1 region and the linker region connecting domains II and III.

*2: Y336F was ignored because an identical substitution is found in human calpain 10.

*3: The I405V substitution is found in mouse p94.

*4: N449D was ignored because an identical substitution is found in two nematode calpains and plant calpains.

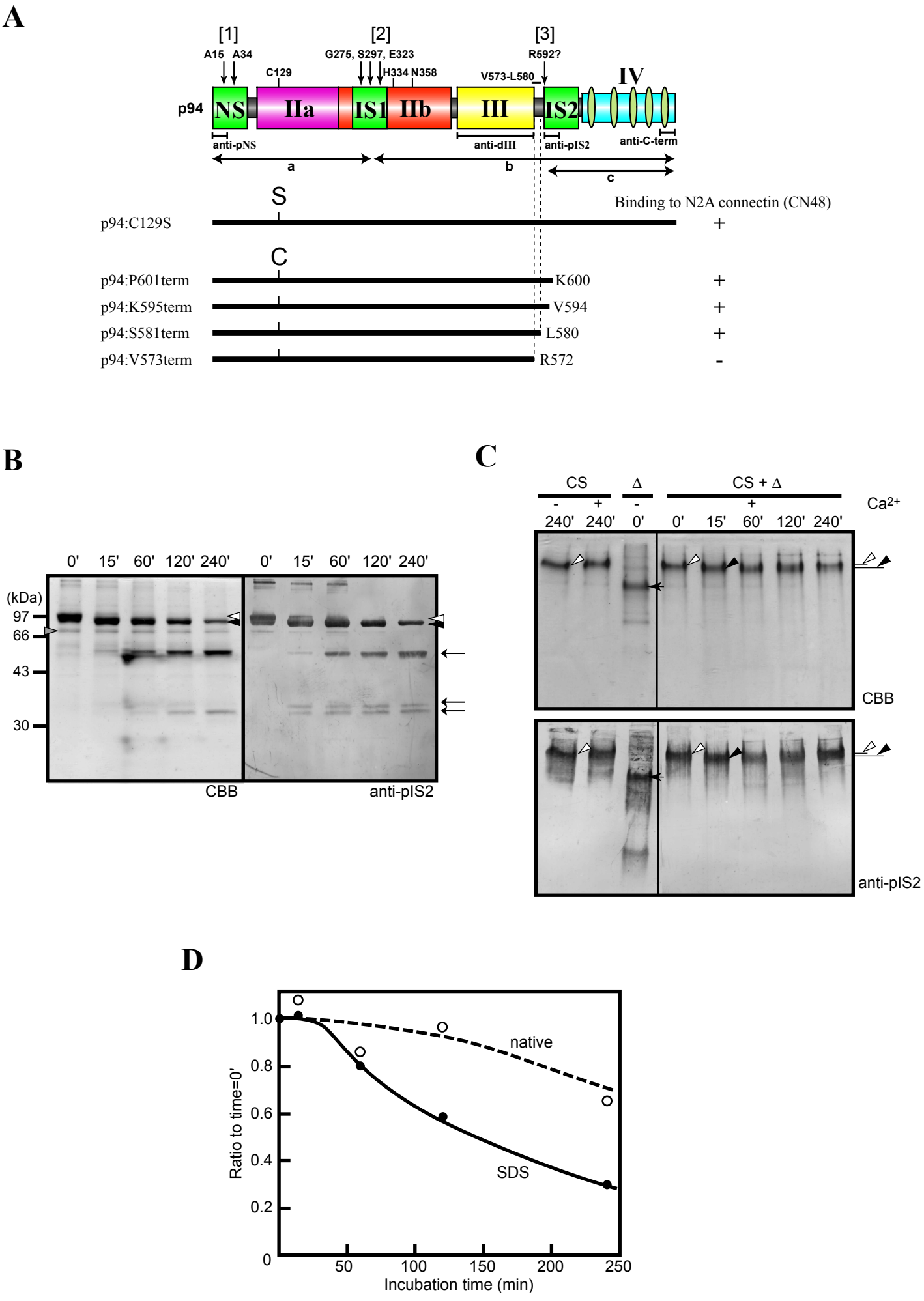
A
[1]
[2]
[3]
A15 A34
C129
G275, S297, E323
H334 N358
R592?
V573-L580
IV
p94
NS
IIa
IS1
IIb
III
IS2
anti-pNS
anti-dIII
anti-pIS2
anti-C-term
a
b
c
S
Binding to N2A connectin (CN48)
p94:C129S
+
C
p94:P601term
K600
+
p94:K595term
V594
+
p94:S581term
L580
+
p94:V573term
R572
-
B
0' 15' 60' 120' 240' 0' 15' 60' 120' 240'
(kDa)
97
66
43
30
CBB
anti-pIS2
C
CS
Δ
CS + Δ
Ca2+
- + - +
240' 240' 0' 0' 15' 60' 120' 240'
CBB
anti-pIS2
D
Ratio to time=0'
1.0
0.8
0.6
0.4
0.2
0
native
SDS
50
100
150
200
250
Incubation time (min)

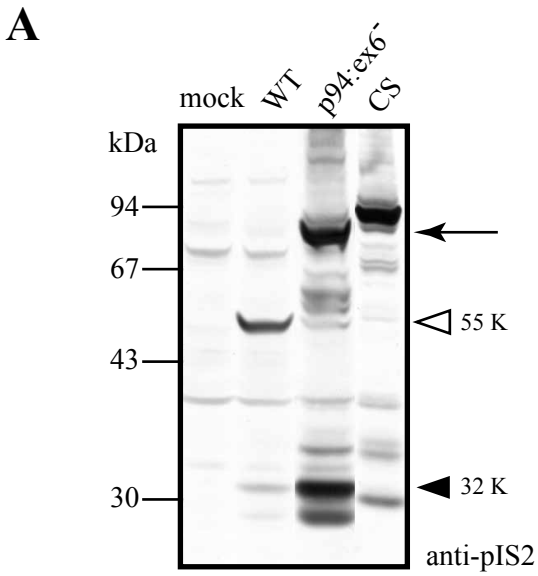
A
mock
WT
p94:ex6⁻ CS
kDa
94
67
43
30
55 K
32 K
anti-pIS2

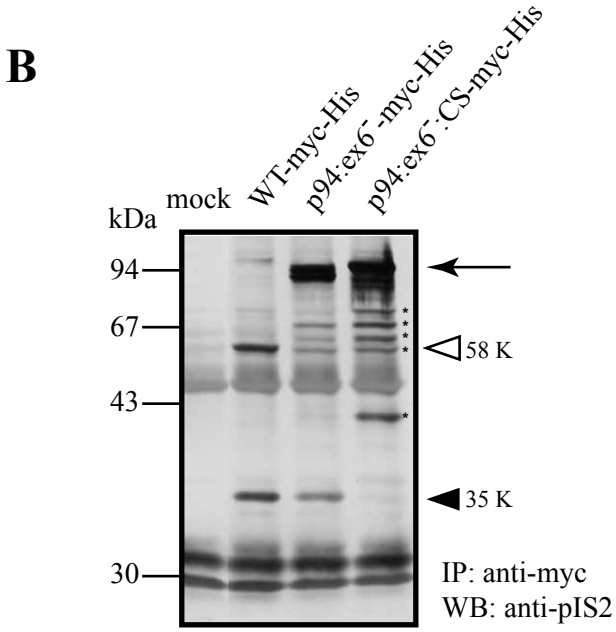
B
mock
WT-myc-His
p94:ex6⁻-myc-His
p94:ex6⁻:CS-myc-His
kDa
94
67
43
30
58 K
35 K
IP: anti-myc
WB: anti-pIS2

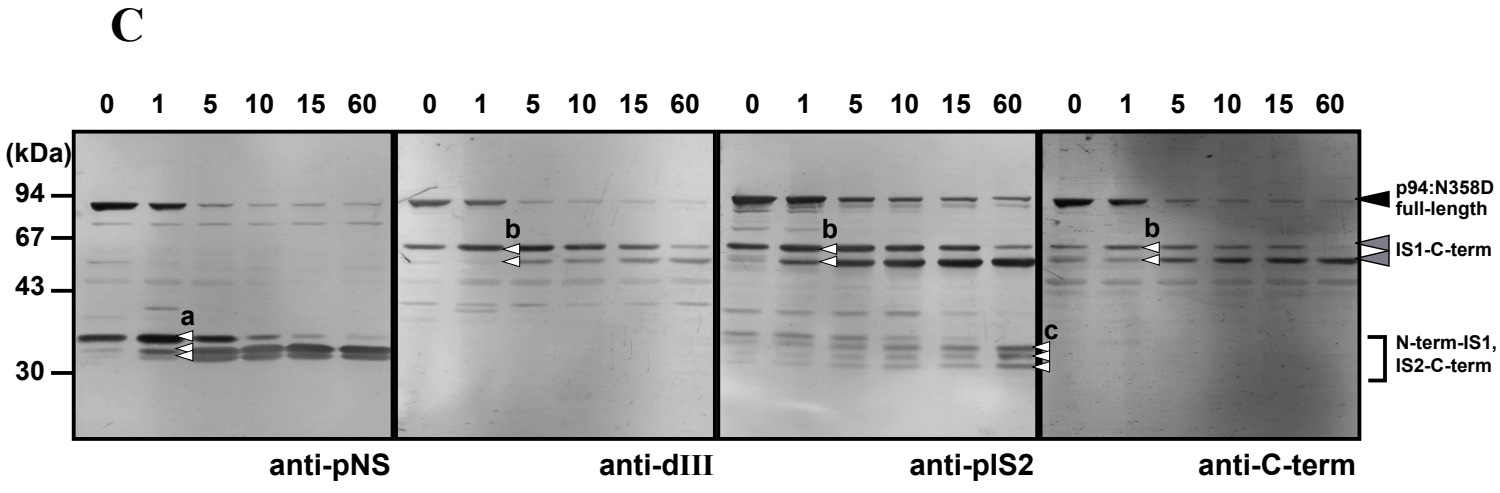
C
0 1 5 10 15 60 0 1 5 10 15 60 0 1 5 10 15 60 0 1 5 10 15 60
(kDa)
94
67
43
30
a
b
b
b
c
p94:N358D full-length
IS1-C-term
N-term-IS1, IS2-C-term
anti-pNS
anti-dIII
anti-pIS2
anti-C-term

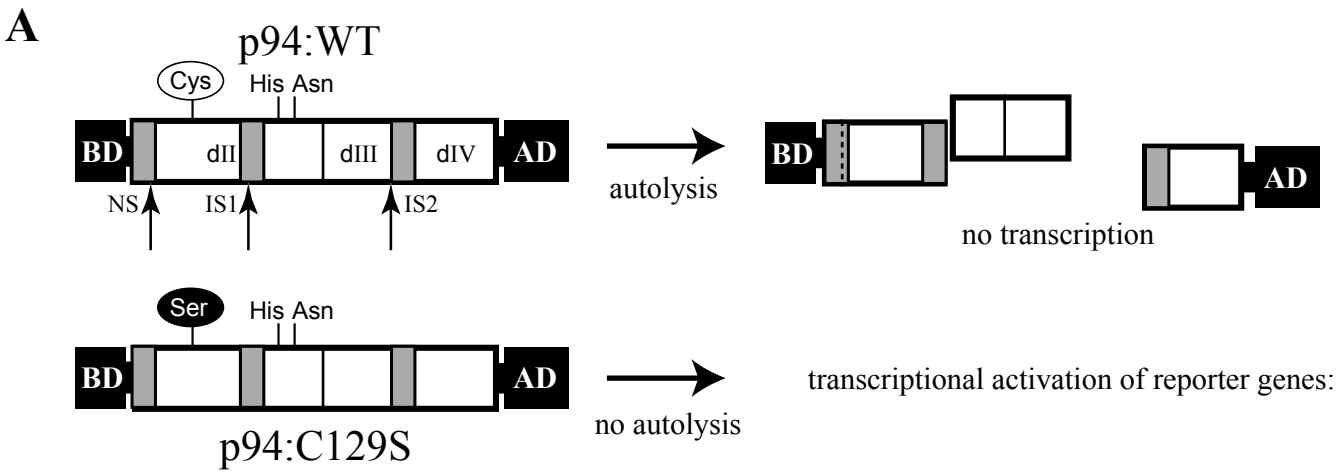
A
p94:WT
Cys
His Asn
BD
dII
dIII
dIV
AD
NS
IS1
IS2
autolysis
BD
AD
no transcription
Ser
His Asn
BD
AD
p94:C129S
no autolysis
transcriptional activation of reporter genes:

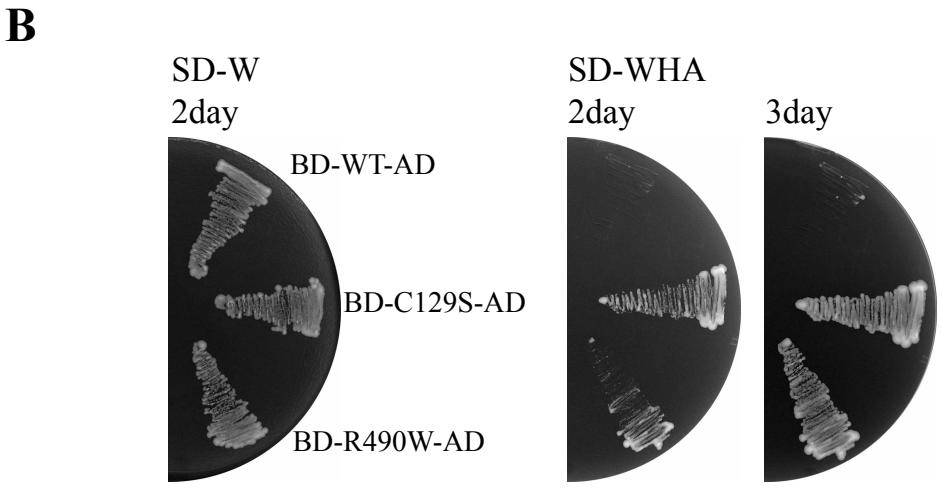
B
SD-W
2day
SD-WHA
2day
3day
BD-WT-AD
BD-C129S-AD
BD-R490W-AD

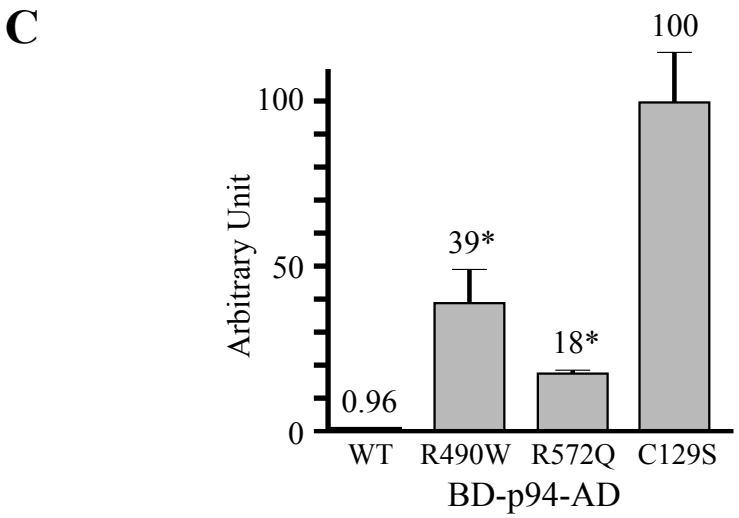
C
100
100
39*
18*
0.96
50
0
Arbitrary Unit
WT
R490W
R572Q
C129S
BD-p94-AD

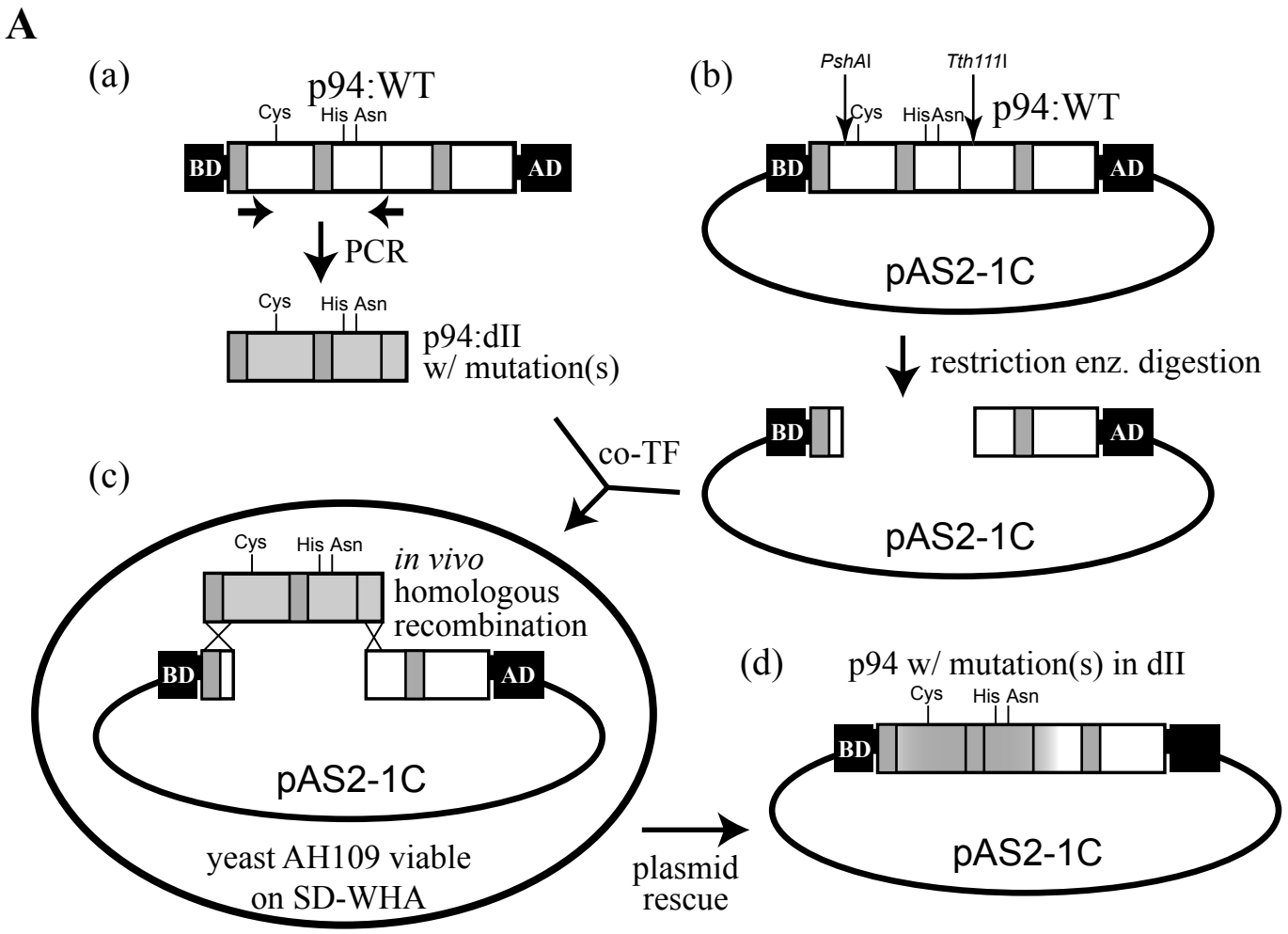
A
(a)
p94:WT
Cys
His Asn
BD
AD
PCR
p94:dII
w/ mutation(s)
(b)
PshAI
Tth111I
p94:WT
pAS2-1C
restriction enz. digestion
co-TF
(c)
in vivo
homologous
recombination
yeast AH109 viable
on SD-WHA
(d)
p94 w/ mutation(s) in dII
plasmid
rescue

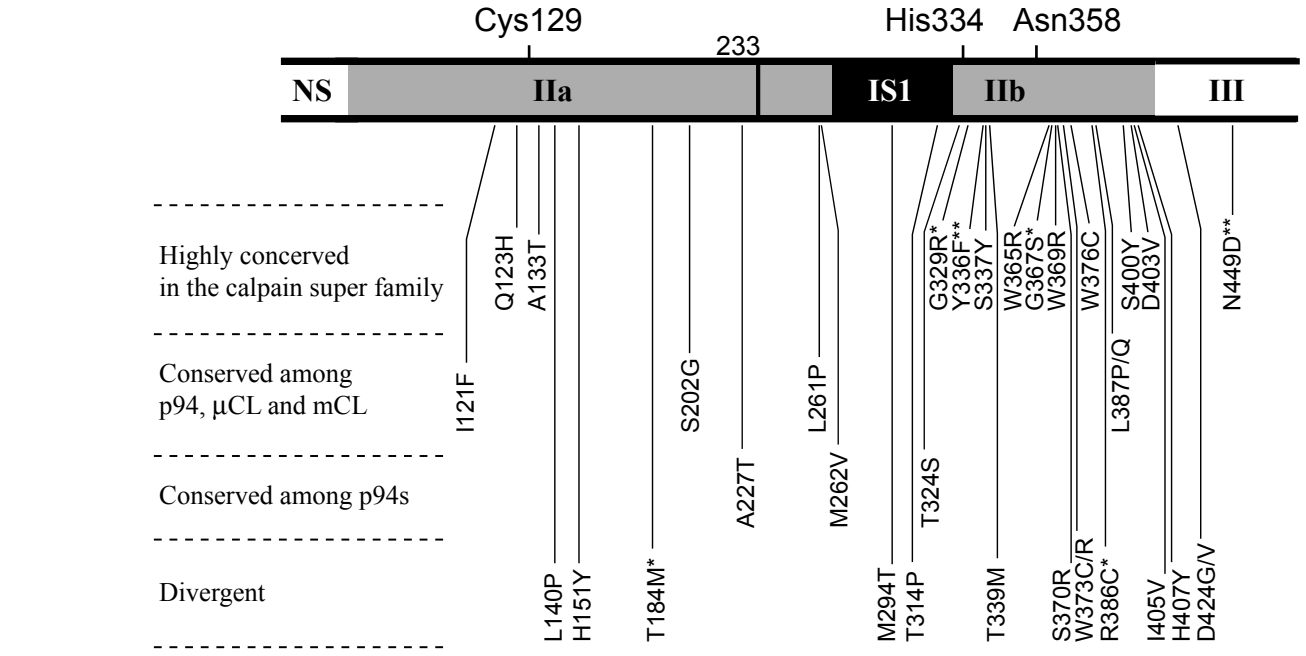
B
Cys129
His334
Asn358
233
NS
IIa
IS1
IIb
III
Highly concerved
in the calpain super family
Conserved among
p94, μCL and mCL
Conserved among p94s
Divergent
I121F
Q123H
A133T
L140P
H151Y
T184M*
S202G
A227T
L261P
M262V
M294T
T314P
T324S
G329R*
Y336F**
S337Y
T339M
W365R
G367S*
W369R
S370R
W373C/R
W376C
R386C*
L387P/Q
S400Y
D403V
I405V
H407Y
D424G/V
N449D**

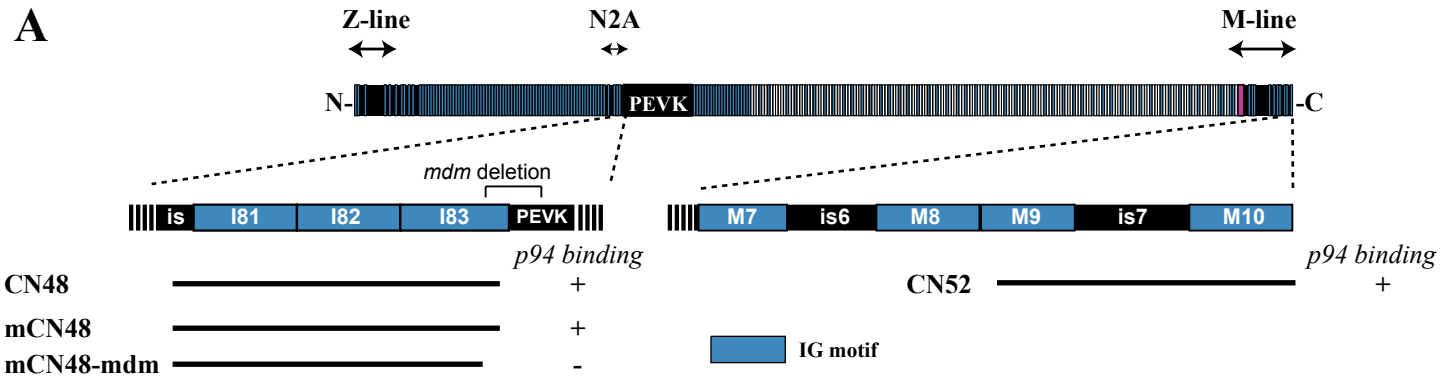
A
Z-line
N2A
M-line
N-
PEVK
-C
mdm deletion
is
I81
I82
I83
PEVK
M7
is6
M8
M9
is7
M10
p94 binding
p94 binding
CN48
+
CN52
+
mCN48
+
mCN48-mdm
-
IG motif

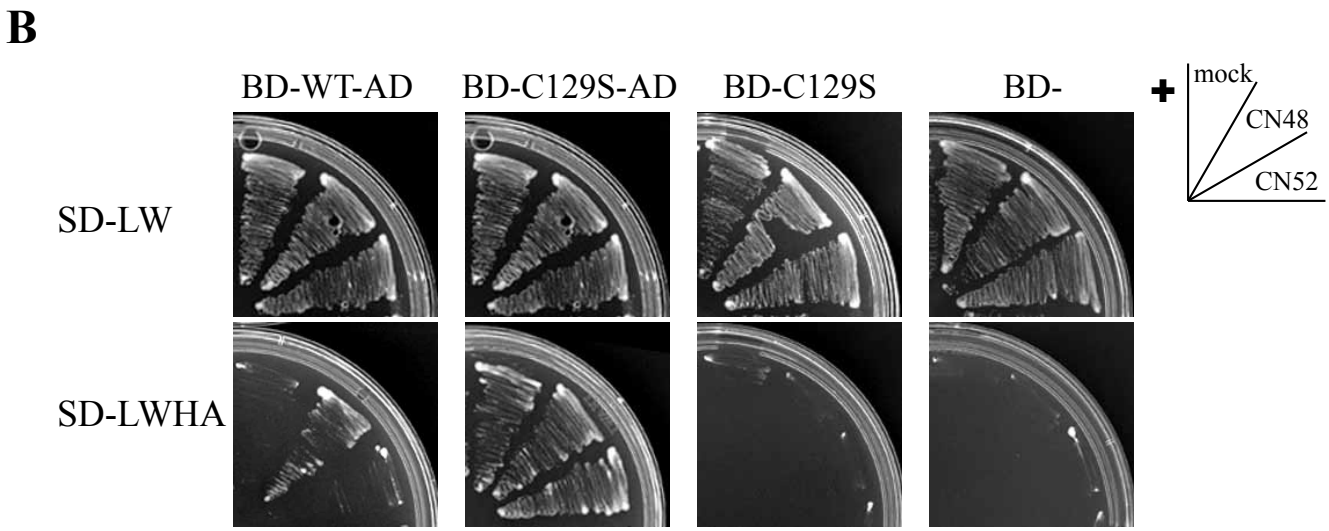
B
BD-WT-AD
BD-C129S-AD
BD-C129S
BD-
+
mock
CN48
CN52
SD-LW
SD-LWHA

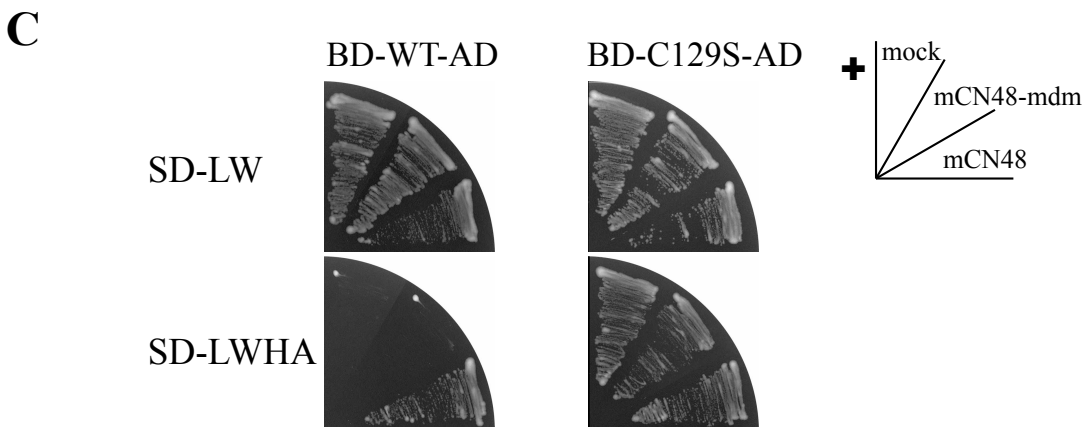
C
BD-WT-AD
BD-C129S-AD
+
mock
mCN48-mdm
mCN48
SD-LW
SD-LWHA

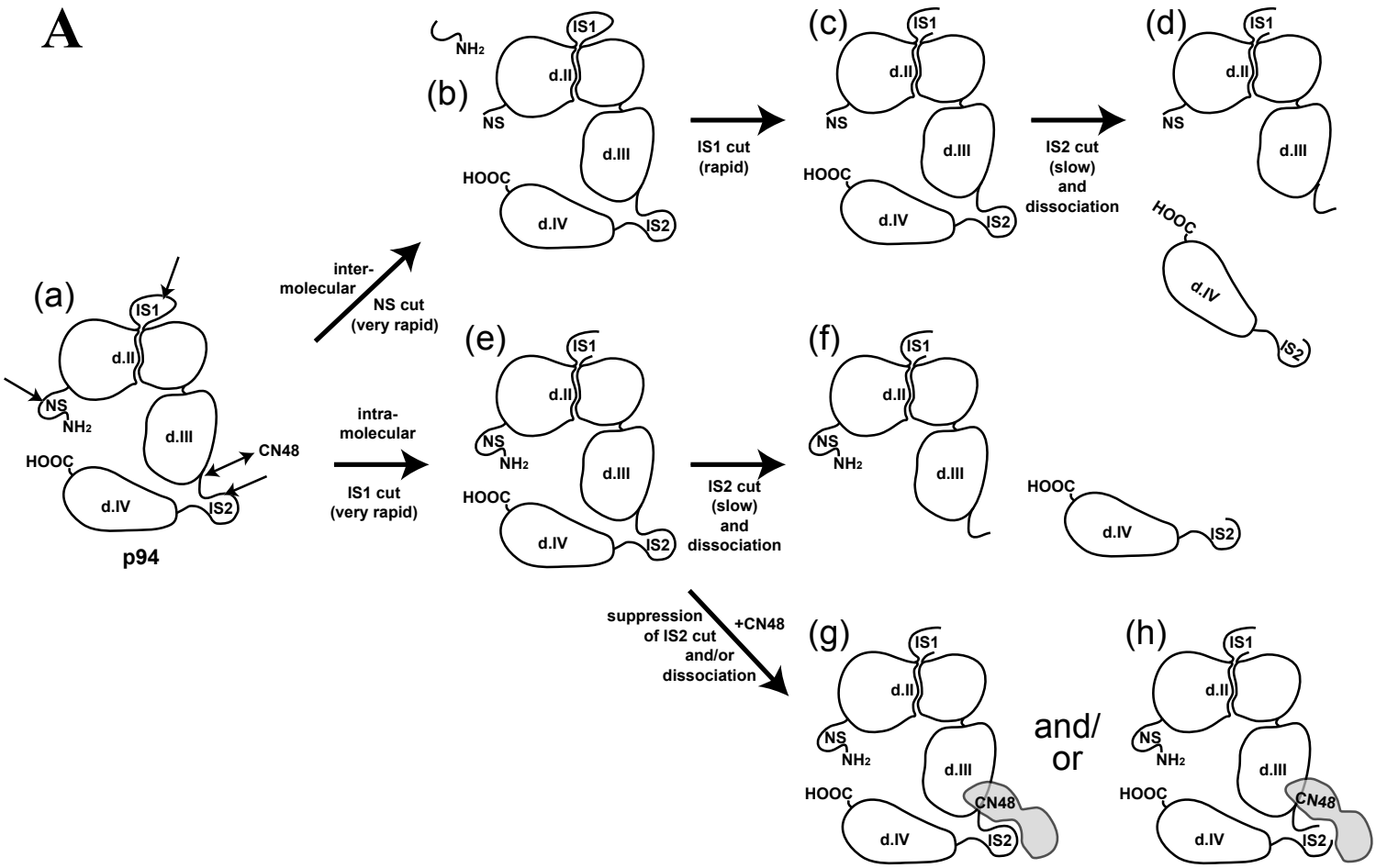
A
(a)
IS1
d.II
NS
NH2
d.III
CN48
HOOC
d.IV
IS2
p94
inter-
molecular
NS cut
(very rapid)
intra-
molecular
IS1 cut
(very rapid)
(b)
(c)
(d)
(e)
(f)
(g)
(h)
IS1 cut
(rapid)
IS2 cut
(slow)
and
dissociation
suppression
of IS2 cut
and/or
dissociation
+CN48
and/
or

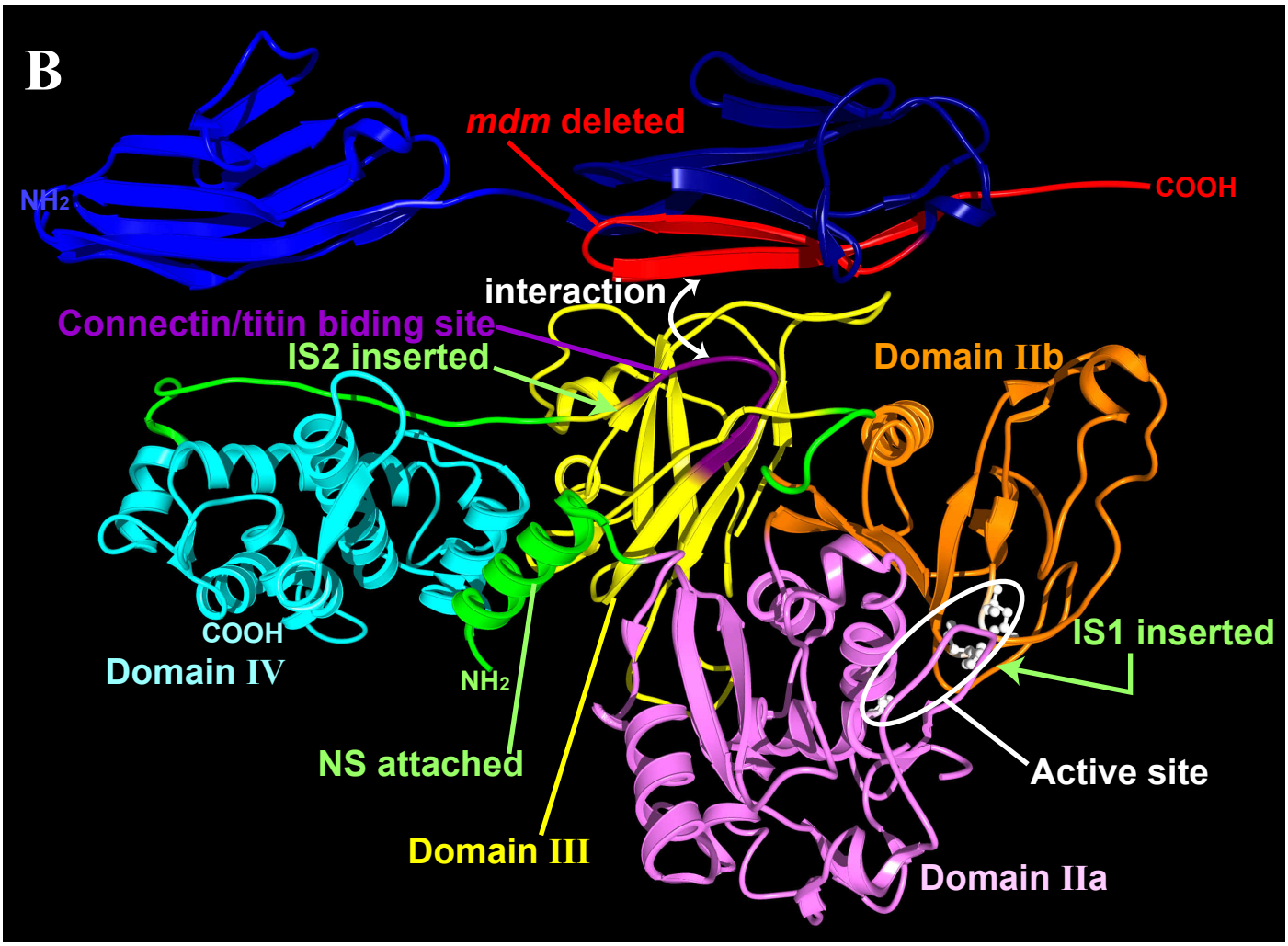
B
mdm deleted
NH2
COOH
interaction
Connectin/titin biding site
IS2 inserted
Domain IIb
COOH
Domain IV
NH2
IS1 inserted
NS attached
Active site
Domain III
Domain IIa